

Parusharamulu Buduma¹ / Gayadhar Panda¹

LQR Based Control Method for Grid Connected and Islanded DG System

¹ Electrical Engineering Department, National Institute of Technology Meghalaya, Shillong, India, E-mail: sp.parasu@gmail.com, p_gayadhar@yahoo.com

Abstract:

This paper presents an output and state feedback robust LQR (OSRLQR) optimal controller for the control of active (P) and reactive power (Q) in grid-connected mode, and voltage (V) and active power in islanded mode of photovoltaic (PV) distributed generation (DG) system. The OSRLQR scheme is comprising of an output and state feedback controllers, which are designed based on LMI-LQR optimization approach. The DG inverter along with proposed controller is configured to work as a current source in grid-connected mode and a voltage source in island mode using P-Q and P-V control scheme respectively. A seamless transition between the grid connected and island modes under the presence of the proposed controller is achieved using a passive island detection and synchronization algorithm along with load shedding. The entire control scheme of the DG system is modelled and analyzed using MATLAB/SIMULINK/Robust Tool-Box, and the practical feasibility of the proposed control scheme is verified using dSPACE. A superior trade-off robustness among the stability and performance is the final outcome of the DG system with proposed control scheme. Performance of the proposed control scheme is compared with conventional PI controller and the comparative results indicate the superior performance of proposed control scheme over the conventional control scheme.

Keywords: distributed generation, photovoltaic systems, robust optimal control, linear quadratic regulator, linear matrix inequality, grid connected and Islanded DG system

DOI: 10.1515/ijeps-2018-0027

Received: January 15, 2018; **Revised:** June 8, 2018; **Accepted:** July 15, 2018

1 Introduction

In the recent past, there is an increase in the distributed power generation due to its low environmental impact and technical advantages. Among these distributed power generation, solar photovoltaic (PV) is a well-established technology but the control of this system in grid connected and islanded modes is a big challenging task. The use of power converters for the DG system allows an independent active and reactive power control of DG system [1]. The basic function of these power converters is to convert the DC input to AC output with desired voltage magnitude and frequency. The desired AC output is obtained by controlling the gain of the voltage source inverter (VSI) which is achieved by Pulse Width Modulation technique (PWM) technique with suitable control method. The quality of the AC output waveform is more important than the quantity and it can be achieved by using the various PWM techniques. The Sinusoidal PWM technique is one of the most prominent technique for DG inverter to reduce the harmonics in the response [2].

The input side of the VSI is controlled by DC-DC boost converter, with the main property to extract the maximum power from the PV system. Maximum Power Point Tracking (MPPT) technique is the most important factor in PV system to extract the maximum available power, reduce the cost. Different MPPT techniques have been explained in [3]. The harmonics present in the inverter output can be smooth-out by the passive or active filter. There is vast literature about the importance of the active and passive filter in [4]–[6]. The advantages of the passive filter to reduce the inverter harmonic over the active filter and the design procedure of passive LCL filter including resonance damping is proposed in [7], however losses in damping component is unacceptable. The passive LCL filter can not only attenuate the harmonics but can also allow the inverter to operate in both islanded mode and grid-connected mode [8].

I. J. Balaguer considered the DG power control as a current source in grid-connected mode and a voltage source in island mode in [9]. The conventional PI current and voltage controller are proposed in dq-reference frame for easy control of active and reactive power. In grid-connected mode, the DG inverter is operated as a current controller to inject preset power to the load and grid. In the islanded mode, the DG inverter is operated

Parusharamulu Buduma is the corresponding author.
© 2018 Walter de Gruyter GmbH, Berlin/Boston.

as voltage controller to maintain the constant reference output voltage. The author also proposed the islanding detection, load shedding and grid synchronization techniques.

Generally a PI controller is employed in the dq-reference frame to acquire the benefits of individual control of active and reactive power. The transformation from abc-reference frame to synchronous rotating dq-reference is achieved by Phase Lacked Loop [10]. In [11]–[13], the authors proposed PI current controller in grid-connected mode, and in [14]&[15], the authors proposed PI voltage controller in islanded mode. However, these methods did not consider the states for control design, the state feedback-based controller gives more stable response for different uncertainties. The PI control can not give robust performance and stability for external and internal disturbances. The resonance uncertainty in LCL filter and current harmonics due to background voltage disturbance are the some of the issues in the conventional controller of LCL filtered inverter, however, the passive LCL filter smooth-out the harmonics produced by the inverter. In [16] author proposed LCL filter with a suitable solution to losses in damping element, however, its performance depends on grid side impedance and extra passive component increase the cost and size. The solution to the current harmonics due to background voltage disturbance is proposed by M. Liserre using rotating frame PI resonance controller in [17], however robustness and filter resonance is not considered. In order to assure the robust performance and stability as well as to contribute a harmonic disturbance and resonance rejection in LCL without using active or passive damping, a robust controller with state feedback have been proposed in [18] & [19], however its performance in terms of resonance damping is still depends on the grid impedance. In order to overcome the above issues this paper uses observer-based state feedback robust LQR optimal controller, and this algorithm considers the output feedback error as one of the states for controller design. The robust LQR controller uses the linear state feedback model. It is accepted that the non-linearities of the PV inverter model are inconsiderable and it has a negligible effect on the system performance and stability [20]. C. Dirscher proposed the state feedback LQR controller in [21], however, LMI approach which gives superior robust performance and stability is not considered. C. Olalla designed the robust LQR controller with an LMI approach in [22], however this design procedure of the robust controller is suitable only for the DC-DC boost converter. J. Douglas proposed robust controller design for the uncertainty in [23], however, the field of application is not related to power converter control. The robust LQR controller with an LMI approach proposed in this research is considered for the DG inverter with LCL filter.

The seamless mode transfer between grid-connected and islanded mode is achieved by using island detection, load shedding and grid synchronization techniques. The island detection technique detects the abnormal conditions and switches the DG from grid-connected mode to island mode while disconnecting from the main grid. Different passive, active and communication-based island detection techniques are proposed by authors in [24]–[27]. Once the normal grid conditions obtained, the DG should reconnect to grid by grid synchronization technique. The grid synchronization technique is proposed by using PLL in [28] & [29]. If the power mismatch occurs between the generation and load when the DG system disconnected from utility grid then there will be excessive variation in voltage and frequency which cannot be sustained for the island operation. In order to limit the variations of the voltage and frequency some part of the load should be disconnected by using load shedding algorithm [30]–[32]. This paper presents the design of an output and state feedback LQR optimal controller with an LMI approach. The OSRLQR controller design involves the output feedback error states and LCL filter states. This OSRLQR controller is used for power control along with the PQ control theory for grid-connected mode and PV control Theory for island mode. In the proposed scheme the DG connects or disconnects to grid with the seamless transition by using a conventional passive island detection algorithm and grid synchronization algorithm along appropriate load shedding in the presence of OSRLQR controller.

The major contributions of this paper are (i) The design of optimal output and state feedback robust controller based on LQR optimization with an LMI approach. (ii) The active and reactive control in the grid-connected mode under the presence of the OSRLQR controller, where the references are generated using DC link voltage control strategy and Reactive power. (iii) The active power and voltage control in island mode, where the references are generated using output voltage and active power. After the introduction, this paper is organized as follows. The system description, modelling, the PQ and PV control theory is explained in Section 2, the controller design procedure is given in Section 3, simulation results and discussions in Section 4 and experimental feasibility of the proposed scheme in Section 5. Finally, Section 6 provides the conclusion of the proposed scheme.

2 The distributed generation system description and modelling

2.1 System description

A PV based DG system used for this research, shown in Figure 1, consist a DC to AC three-phase voltage source inverter (VSI), DC to DC boost converter, battery energy storage system (BESS). The DC to DC boost converter connects the DC-link capacitor at input terminals of the voltage source inverter (VSI). The maximum power point tracker (MPPT) generates the references for the DC to DC boost converter to extract the maximum available at PV system. The MPPT algorithm used in these work is incremental conductance [3]. The inverter convert the DC voltage to AC by using proposed PWM controller scheme and this process is explained in following sections.

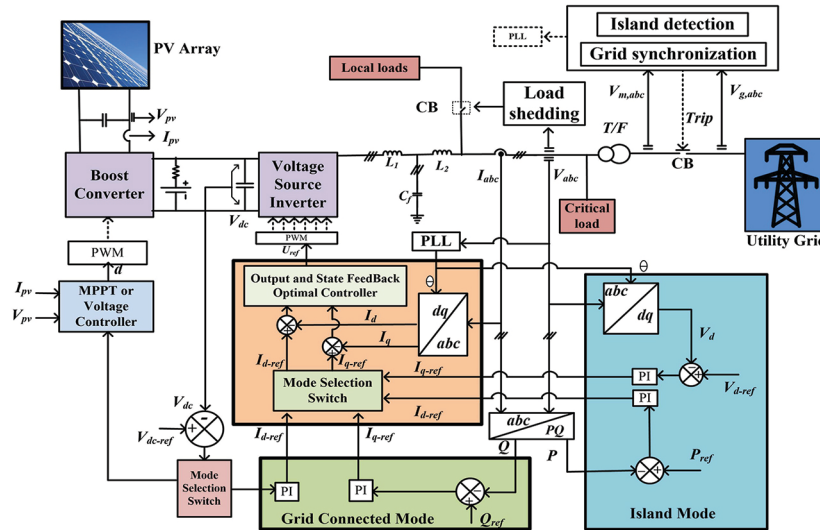


Figure 1: Three phase grid connected and island mode DG system for active and reactive power control with output and state feedback robust LQR optimal controller(OSRLQR).

2.1.1 Sinusoidal PWM technique

The DC side available power is extracted to AC side using the VSI and a suitable PWM control scheme. The VSI convert the DC input voltage to AC output voltage and the output wave forms of the practical VSI are not pure sinusoidal and contains different harmonics. The higher order harmonics can be eliminated using suitable filter at the output of the inverter. The harmonics in the output can be eliminated using high speed inverter with suitable switching techniques. PWM switching techniques are very popular in the field of power electronics. The main objective of the PWM technique is to control the inverter output voltage and to eliminate the harmonics in the output. For all the applications there is no suitable single PWM technique. Sinusoidal and space vector PWM are the some of the important PWM techniques for the VSI. In this research work, a sinusoidal PWM (SPWM) technique is used along with proposed robust LQR controller. Better sinusoidal output waveform can be achieved by using a high switching frequency and by varying the amplitude and frequency of reference voltage in SPWM technique. Figure 2 represents the SPWM technique with proposed robust LQR control signal generation. The dq-frame control signal is generated with robust LQR controller and it can be converted to suitable reference abc-frame by using DQ-PLL. In this research work, the triangular wave as a carrier signal and sine wave as a reference signal are used to generate the pulses to the converter by the comparison method with help of comparator. The switching devices are placed in each leg of the full bridge inverter as pair like $S_1 - S_4$, $S_3 - S_6$ and $S_5 - S_2$. A sample output pulses generated for switch pair $S_1 - S_4$ using SPWM technique are shown in Figure 2.

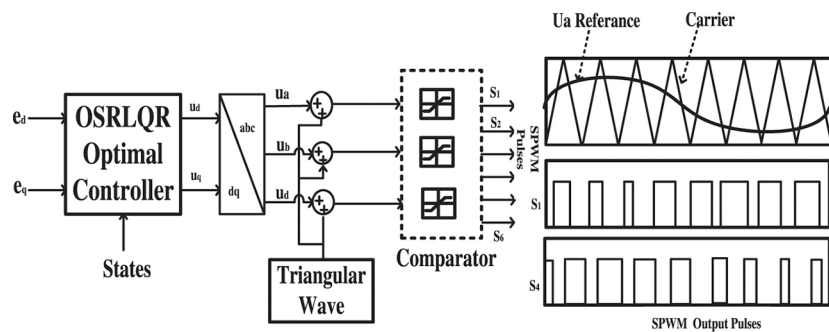


Figure 2: Sinusoidal PWM technique along with proposed robust LQR controller.

2.1.2 LCL-Filter design

The output of the VSI is smoothed out from the harmonics using passive LCL filter. The LCL filter is gaining more advantages over the L filter for the VSI due to its smaller size, lower cost, better dynamics and higher attenuation. The characteristics considered for the design of the passive LCL filter are the current ripple, filter size, switching ripple attenuation and resonance. The design procedure of LCL filter is considered as in [7]. The LCL filters reduce the current or voltage harmonics produced due to PWM switching action, to a certain acceptable harmonic level. The main issues with LCL filtered conventional controller of VSI are background voltage harmonics and resonance of the LCL filter. The state feedback robust controller damp out the resonance problem occurs in LCL filter due to parameter variations without using active or passive damping and rejects the current harmonic distortions due to background voltage disturbance.

2.2 Control strategy of DG inverter system

The outer control loop of the VSI generates the references for inner control loop using P-Q control techniques in grid-connected mode and P-V control techniques in islanded mode as shown in Figure 1. In the grid-connected mode, the DC-link voltage V_{dc} is maintained constant by voltage controller while controlling the available active power and this process generates the current reference for the current controller of the VSI. In the islanded mode the DC-link voltage V_{dc} is maintain constant by DC side voltage control and MPPT while extracting the maximum available power from PV system. This process generates the references for the DC to DC boost converter and no explanation is considered in this paper about the DC side control except DC link voltage as the assumption of fully stabilized DC system. The references for the inverter in island mode are generated by output voltage and active power control as in [15]. The VSI has a prime control objective to transfer the power extracted from the boost stage to the load and grid. The VSI control method used to achieve the objective of this research is a novel robust controller. The novel robust controller is designed using LQR optimization including LMI constraints. The DG system with proposed robust controller acts as a voltage source in the island mode and current source in the grid-connected mode. The mode selection switch shown in Figure 1, switches the control operation from grid-connected mode to island mode and vice-versa based on the signal received from island detection algorithm. For the easy control of the active and reactive power, the three-phase system dynamics are reduced to a two-phase d-q reference frame instead of the three abc reference frame. The synchronous d-q reference frame is obtained from the three abc reference frame using a conventional phase locked loop (PLL) which is designed based on a synchronous reference frame (SRF) as in [10].

2.2.1 Proposed control description

The desired features of the robust controller: (i) good tracking of the references, (ii) reduction of resonance and harmonic disturbances and (iii) stability for the internal and external uncertainty. In order to achieve the above feature, an OSRLQR controller is considered in the inner loop of this research and design procedure is given in Section 3. The robust control design procedure utilizes the variables of LCL filter and the output current error as states. The states of the LCL filter obtained using state observer and this observer design method is explained in Section 3.2. The proposed OSRLQR controller is designed using LQR optimization including LMI constraints in Section 3.4.

2.3 Active and reactive power control in grid-connected mode

The active and reactive power control is achieved by the outer control loop with PQ control theory which generates the references for the inner control loop. The optimal output feedback controller is used to minimize the error in the current. The measured current and voltage at PCC (i_{abc} and v_{abc}) are converted into dq frame with park transformation. The i_d component of current is controlled to manage the active power and i_q component of current is controlled to manage the reactive power. Thus, the active power and reactive power is calculated separately as

$$P = \frac{3}{2}(v_d i_d + v_q i_q) \quad (1)$$

$$Q = \frac{3}{2}(v_q i_d - v_d i_q) \quad (2)$$

Assuming the grid current vector is in phase with grid voltage than the $v_q = 0$. Therefore, the active and reactive power respectively as follows

$$P = \frac{3}{2}(v_d i_d) \quad (3)$$

$$Q = \frac{3}{2}(-v_d i_q) \quad (4)$$

it can be inferred that the active power injected into the grid is directly dependant on the d-axis current (I_d). in this work the I_{d-ref} is generated using the DC link voltage controller as shown in Figure 1. The current requirement for reactive power compensation (I_r) is a function of the voltage sag v_{sag} . The maximum apparent power $|S| = (|v_a|_{rms} + |v_b|_{rms} + |v_c|_{rms})I_{max}$. where I_{max} is the maximum current limit then the reference reactive power (Q_{ref}) can be expressed as

$$Q_{ref} = |S|I_r \quad (5)$$

Using the Q_{ref} and Q, I_{q-ref} is generated as shown in Figure 1. The I_{d-ref} and I_{q-ref} thus generated are given to the OSRLQR for the further tracking.

2.4 Island detection and load shedding

The island detection algorithm detect the variations in grid voltage and frequency and send the signal to circuit breaker to isolates the DG system from the grid during abnormal conditions. The different active, passive and communication based island detection are discussed in literature. The active and communication based island detection techniques are not economical. A conventional passive island detection method is implemented in this research work as in [9]. The algorithm sends a signal for mode selection switch and circuit breaker for isolating the DG system to facilitate a suitable switching in the control. The instant at which the DG is cut off from the main grid (islanding operation) must be detected in order for the DG system to change between grid-connected and islanding modes. This detection is achieved by using a DQ-PLL (SRF-PLL) which consists of Clarkes transformation and provide the voltage (V_d) and frequency (f) from measured voltage V_{abc} . The schematic of the DQ-PLL is realized by setting Vq to zero. A PI regulator can be used to control this variable, and the output of this regulator is the grid frequency. In addition to the frequency, the DQ-PLL is capable of tracking the magnitude of its input signals. These two parameters, namely, frequency and voltage magnitude, are used in the islanding detection algorithm to detect the grid condition and the algorithm is shown in Figure 3 (a). The algorithm sends a signal that switches the inverter to the suitable interface control.

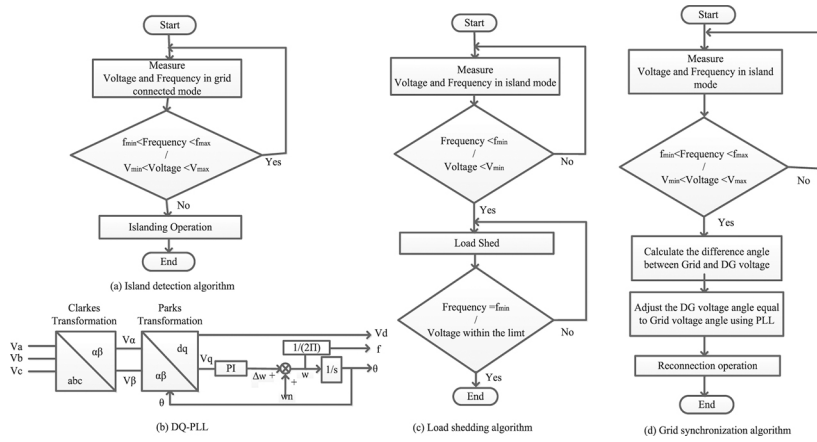


Figure 3: The transition techniques between grid connected and islanded modes (a) Island detection algorithm, (b) dq-PLL, (c) Load shedding algorithm, (d) Grid synchronization algorithm.

In grid-connected mode, the main utility grid will supply the difference between the DG and load power, but in island mode, this difference power cannot be supplied by the utility which may result in voltage and frequency transients at the load. Hence, a proper load shedding should be done in order to maintain the load voltage and frequency within the limits. The process by which some portion of the load is disconnected to avoids the transients in voltage and frequency when the main grid disconnected is called load shedding. The island detection is not enough for islanding operation because the DG source may not supply the total local load demand, hence a load shedding is required. If there is a deviation in normal voltage and frequency range in the island mode of system after connecting to the voltage control mode, then the load shedding algorithm gives the signal for the circuit breaker for disconnect the some part of the load. The load shedding technique is implemented in this work as in [31] and the algorithm is shown in Figure 3 (c).

2.5 Active power and voltage control in Island mode

The control scheme in island mode has two loops that are inner and outer loops. The inner loop controls the load current transients, whereas the outer loop controls the active power fed to load and voltage magnitude at the load terminal in island mode [15].

Active power control: The measured active power (P) from eq. (3) and P_{ref} are used to generate the I_{d-ref} for the inner OSRLQR controller shown in Figure 1. The P_{ref} is given by

$$P_{ref} = |S|(1 - I_r) \quad (6)$$

Voltage control: In this control scheme, a PLL adjusts the q-axis voltage component to zero, PLL forces the d-axis voltage to the reference voltage vector (terminal voltage) that means q-axis component of the output voltage is zero. The q-axis current from the inverter given by

$$I_q = -(v_d w L_L) / (1.5(R_L^2 + (w L_L^2))) \quad (7)$$

This suggests that q-axis current of the inverter is proportional to the d-axis voltage. The control for regulating d-axis voltage is as follows

$$I_{qref} = (K_p + K_I/s)(V_{ref} - V) \quad (8)$$

The I_{qref} generated by the outer loop is given to OSRLQR controller. This scheme controls the output voltage and limits the overcurrent in island mode.

2.6 Grid synchronization algorithm

When the voltage and frequency variations disappear in the grid, the re-connection process from island mode to grid-connected mode can be initiated. To nullify the transients while reconnecting, the DG voltage magnitude and phase angle is to be perfectly synchronized with grid voltage magnitude and phase angle. The phase angle adjustment is achieved by PLL. When the DG Voltage is synchronized with grid voltage then the DG is re-connected to grid and the synchronization algorithm is shown in Figure 3 (d). The synchronization technique send a signal to the mode selection switch to connects DG system to the current control mode from voltage control mode [9].

2.7 Modelling of LCL-filtered inverter-based DG unit

The three-phase DG VSI with LCL filter, operated in a grid-connected and island mode as shown Figure 1 are considered for deriving the state-space model and control design. The controller is designed using the linear state space model which is obtained by state feedback and output feed back variables. The controller design is simple and easy by the use of linear model approach other than nonlinear approach, however the converter dynamics are nonlinear due to its switching characteristics. The main disadvantages of the non-linear controllers are the difficulty to predict transient performances and the complexity of the implementation, however, the design of the controller for the system by neglecting non-linearity may deteriorate the results from the desired. Most of the authors have adapted linear robust control techniques besides of non-linear control to achieve the robust stability under different operating conditions. In this research, we will use linear controller which is designed based on LQR technique along LMI constraints which is called OSRLQR controller. Due to the robust nature of the OSRLQR controller, the desired performance is achieved even for neglecting the model non linearity. R.Prez Ibacacho proposed a state model by neglecting the non linearity and the effect of the model non linearity on control design [20]. The linearized model of the three phase VSI with LCL filter for the design of OSRLQR controller is obtained by the state variables of the system. The V_{abc} is the three-phase output voltage of the DG system at the point of common coupling (PCC). The current through inductor and voltage across the capacitor of the system are the state variables for the observer design. The three-phase system dynamics are reduced to a two-phase d-q reference frame instead of the three abc-reference frame. Hence the dynamic state vector for the observer design is expressed as

$$\mathbf{x}(t) = [i_{1d}(t) \ i_{1q}(t) \ i_{2d}(t) \ i_{2q}(t) \ V_{cd}(t) \ V_{cq}(t)]^T \quad (9)$$

The inductor currents, capacitor voltage and output current error of the system are the state variables for the controller design of the grid connected and the island mode. Hence the dynamic state vector for LQR controller design expressed as

$$\mathbf{x}(t) = [i_{1d}(t) \ i_{1q}(t) \ i_{2d}(t) \ i_{2q}(t) \ V_{cd}(t) \ V_{cq}(t) \ e_d(t) \ e_q(t)]^T \quad (10)$$

where $v_1(t)$ is the converter side voltage and $v_2(t)$ is grid side voltage. The variations of the output voltage $v_2(t)$ are considered as external disturbance for the controller design.

2.7.1 State space model of DG system

The dynamic equations of the DG inverter system with LCL filter in abc-frame are as follows

$$di_1^{abc}(t)/dt = [(v_1^{abc}(t) - v_c^{abc}(t) - R_f(i_1^{abc}(t) - i_2^{abc}(t)) - R_1 i_1^{abc}(t))/L_1] \quad (11)$$

$$di_2^{abc}(t)/dt = [(v_c^{abc}(t) - v_2^{abc}(t) + R_f(i_1^{abc}(t) - i_2^{abc}(t)) - R_2 i_2^{abc}(t))/L_2] \quad (12)$$

$$dV_c/dt = (i_1^{abc}(t) - i_2^{abc}(t))/c \quad (13)$$

$$de^{abc}/dt = i_r^{abc}(t) - i_2^{abc}(t) \quad (14)$$

The dynamic equations in dq-refarance frame with decoupling are given in following equations

$$di_{1d}(t)/dt = [v_{1d}(t) - v_{cd}(t) - R_f(i_{1d}(t) - i_{2d}(t)) - R_1 i_{1d}(t)]/L_1 + w_g i_{1q}(t) \quad (15)$$

$$di_{1q}(t)/dt = [v_{1q}(t) - v_{cq}(t) - R_f(i_{1q}(t) - i_{2q}(t)) - R_1 i_{1q}(t)]/L_1 - w_g i_{1d}(t) \quad (16)$$

$$\mathbf{A} = \begin{pmatrix} -(R_1 + R_f)/L_1 & w_g & R_f/L_1 & 0 & (-1)/L_1 & 0 & 0 & 0 \\ -w_g & -(R_1 + R_f)/L_1 & 0 & R_f/L_1 & 0 & (-1)/L_1 & 0 & 0 \\ R_f/L_2 & 0 & -(R_2 + R_f)/L_2 & w_g & 1/L_2 & 0 & 0 & 0 \\ 0 & R_f/L_2 & -w_g & -(R_2 + R_f)/L_2 & 0 & 1/L_2 & 0 & 0 \\ 1/C & 0 & -1/C & 0 & 0 & w_g & 0 & 0 \\ 0 & 1/C & 0 & -1/C & -w_g & 0 & 0 & 0 \\ 0 & 0 & -1 & 0 & 0 & 0 & 0 & 0 \\ 0 & 0 & 0 & -1 & 0 & 0 & 0 & 0 \end{pmatrix}$$

$$di_{2d}(t)/dt = (v_{cd}(t) - v_{2d}(t) + R_f(i_{1d}(t) - i_{2d}(t)) - R_2 i_{2d}(t)/L_2 + w_g i_{2q}(t)) \quad (17)$$

$$di_{2q}(t)/dt = (v_{cq}(t) - v_{2q}(t) + R_f(i_{1q}(t) - i_{2q}(t)) - R_2 i_{2q}(t)/L_2 - w_g i_{2d}(t)) \quad (18)$$

$$dV_{cd}(t)/dt = (i_{1d}(t) - i_{2d}(t))/c \quad (19)$$

$$dV_{cq}(t)/dt = (i_{1q}(t) - i_{2q}(t))/c \quad (20)$$

and two more state equations of current error are required for the design of the robust LQR controller as follows

$$de_d(t)/dt = i_{rd}(t) - i_{2d}(t) \quad (21)$$

$$de_q(t)/dt = i_{rq}(t) - i_{2q}(t) \quad (22)$$

The state space model of the system

$$\dot{\mathbf{x}}(\mathbf{t}) = \mathbf{A}\mathbf{x}(\mathbf{t}) + \mathbf{B}_1\mathbf{u}_1(\mathbf{t}) + \mathbf{B}_2\mathbf{u}_2(\mathbf{t}) \quad (23)$$

$$\mathbf{y}(\mathbf{t}) = \mathbf{C}\mathbf{x}(\mathbf{t}) \quad (24)$$

where $u_1(t) = v_1(t)$ represent the input, $u_2(t) = v_2(t)$ represent the disturbance and $y(t) = i_2(t)$.

The state space matrices for the design of inner loop the robust LQR controller.

$$\mathbf{B}_1 = \begin{pmatrix} 1/L_1 & 0 \\ 0 & 1/L_1 \\ 0 & 0 \\ 0 & 0 \\ 0 & 0 \\ 0 & 0 \\ 0 & 0 \\ 0 & 0 \end{pmatrix} \quad \mathbf{B}_2 = \begin{pmatrix} 0 & 0 \\ 0 & 0 \\ -1/L_2 & 0 \\ 0 & -1/L_2 \\ 0 & 0 \\ 0 & 0 \\ 0 & 0 \\ 0 & 0 \end{pmatrix} \quad \mathbf{C} = \begin{pmatrix} 0 & 0 & 1 & 0 & 0 & 0 & 0 & 0 \\ 0 & 0 & 0 & 1 & 0 & 0 & 0 & 0 \end{pmatrix}$$

The state space model of the system

$$\dot{\mathbf{x}}(\mathbf{t}) = \mathbf{A}\mathbf{x}(\mathbf{t}) + \mathbf{B}\mathbf{u} \quad (25)$$

$$\mathbf{y}(\mathbf{t}) = \mathbf{C}\mathbf{x}(\mathbf{t}) \quad (26)$$

where $\mathbf{B} = [\mathbf{B}_1 \mathbf{B}_2]$ and $\mathbf{u} = [\mathbf{u}_1 \mathbf{u}_2]^T$. The variations in $u_2 = V_2$ are considered as the external disturbance. The disturbance in PCC voltage may be due to the load changes and grid changes. The matrix B_2 indicates the external uncertainty. The elements involved in the state space matrices may depend on internal and external uncertain. Then, the state space model can be expressed as a function of these uncertainties

$$\dot{\mathbf{x}}(\mathbf{t}) = \mathbf{A}(p)\mathbf{x}(\mathbf{t}) + \mathbf{B}(p)\mathbf{u}(\mathbf{t}) \quad (27)$$

where p is the uncertainty vector with n number of uncertainties as $p = (p_1, p_2, \dots, p_n)$, and each uncertain parameter p_i is bounded between a minimum (p_{i-min}) and maximum (p_{i-max}) value as $p_i \in [p_{i-min}, p_{i-max}]$. The robust LQR controller is designed in section 3.4 for the inner current control loop using the above state space matrices.

3 Output and state feedback robust LQR optimal controller

Optimal control is the branch of control theory that deals with designing controls for dynamic systems by minimizing a performance index that depends on the system state variables. The states of the system are obtained using state observer. The observer and controller are designed if the system model is controllable and observable. The states required for the design of inner loop controller are taken from the state observer. The design procedure of controller for the GMO and IMO is as follows.

3.1 Controllability and observability

Controllability: The system $\dot{x} = Ax + Bu$ and $y = Cx + Du$ is controllable if rank of $[B \ AB \ A^2B \ ... \ A^{(n-1)}B]$ is equal to rank of A . For this system $n=6$ for observer design and $n=8$ for controller design, The rank of $[B \ AB \ A^2B \ ... \ A^{(6-1)}B]$ is equal to rank of A if and only if $L_1 > 0, L_2 > 0, C > 0$ and $L_2 - R_f RC \neq 0$.

Observability: The system $\dot{x} = Ax + Bu$ and $y = Cx + Du$ is observable if rank of $[C^T, (CA)^T, (CA^2)^T \ ... \ (CA^{(n-1)})^T]^T$ is equal to rank of A . The rank of $[C^T, (CA)^T, (CA^2)^T \ ... \ (CA^{(6-1)})^T]^T$ is equal to rank of A if and only if $L_1 > 0, L_2 > 0, C > 0$ and $L_2 - R_f RC \neq 0$.

3.2 Observer design

Definition 1: If the matrix pair (A, B) is controllable then the state feedback control law of the closed-loop system can be defined as $u = -K_1x_1 - K_2x_2 - K_3x_3 \ ... \ - K_nx_n = -Kx$. where $K = [K_1 \ K_2 \ ... \ K_n]$

$$\dot{x} = (A - BK)x \quad (28)$$

The characteristic equation of the system is given as

$$|sI - (A - BK)| = 0 \quad (29)$$

If all the eigen values of $(A - BK)$ are placed in the left half plane then closed loop system is asymptotically stable.

Definition 2: If the matrix pair (A, C) is observable then the system states can be reproduced by the state observer which can be expressed as

$$\dot{\hat{x}} = A\hat{x} + Bu + L(\hat{y} - y) \quad (30)$$

here $\hat{y} = Cx\hat{x} = (A - LC)\hat{x} + Bu + Ly$ there exists a matrix L such that the inequality is solvable for $P > 0$.

$$(A - LC)^T P + P(A - LC) < 0 \quad (31)$$

where P is a positive definite matrix and observer gain matrix is given in

$$L = \begin{pmatrix} L_{11} & L_{12} & L_{13} & L_{14} & L_{15} & L_{16} \\ L_{21} & L_{22} & L_{23} & L_{24} & L_{25} & L_{26} \end{pmatrix}^T \quad (32)$$

The eigen values of the observer can be calculated from the modified characteristic equation is given in eq. (33)

$$|sI - (A - LC)| = 0 \quad (33)$$

The L can be selected such that the eigen values of the matrix $(A - LC)$ are in the stable range.

The observer gives the capacitor voltage and grid side inductor current as states.

3.3 LQR controller

The design of optimal controllers for linear systems with quadratic performance index is called linear quadratic regulator (LQR) problem. The objective of the regulator design is to determine the optimal control law which can transfer the system from its initial state to final state such that a given performance index is minimized. The performance index is selected to give the best trade-off between performance and cost of control. The performance index that is widely used in optimal control design is known as the quadratic performance index and is based on minimum-error and minimum-energy criteria. The LQR controller for the system eq. (25) is obtained by minimizing the performance index

$$J = \int_0^\infty (x^T(t)Qx(t) + u^T(t)Ru(t))dt \quad (34)$$

The control law $u = -Kx(t)$ is the final outcome of LQR controller. where $Q = Q^T$ is state wight matrix and $R = R^T$ is control wight matrix. The controller gain K is obtained by solving the algebraic riccati equation

$$A^T P + PA - PBR^{-1}B^T P + Q = 0 \quad (35)$$

The controller gain \mathbf{K} is obtained by the matrix $\mathbf{P} = \mathbf{P}^T > 0$ as

$$\mathbf{K} = -\mathbf{R}^{-1}\mathbf{B}^T\mathbf{P} \quad (36)$$

The demerits of this normal LQR formulation is that it is valid only for the system without uncertainty. It is the best practice to select these matrices \mathbf{Q} and \mathbf{R} to be diagonal and the diagonal elements are adjusted such that state variables can be controlled to desired values. Therefore, first, select the \mathbf{Q} matrix and then select the \mathbf{R} matrix which is an identity matrix. More weight is given for diagonal entry for good performance. Explicitly, we can select any $\mathbf{Q} = \mathbf{Q}^T > 0$ and then solve the linear equation $\mathbf{A}^T\mathbf{P} + \mathbf{P}\mathbf{A} = \mathbf{Q}$ for the guaranteed positive-definite matrix \mathbf{P} if the system is stable.

The LQR will give some inherent robustness based on the weight matrices \mathbf{Q} and \mathbf{R} selection but it does not give guarantee for enough inherent robustness trade-off among the stability and performance robustness for the any uncertainty occurs in the system. To overcome these drawback a robust LQR is controller is designed using the uncertainty model in the fallowing section.

3.4 The robust LQR control method with an LMI approach

This section deals the detailed procedure of the robust LQR control design method with uncertain model. The Figure 4 shows OSRLQR with system state feedbacks and current error states. Here, we explain the basic idea of robust quadratic stability in the form of LMI. The design procedure of OSRLQR based using LMI constraints is explained considering different uncertainties.

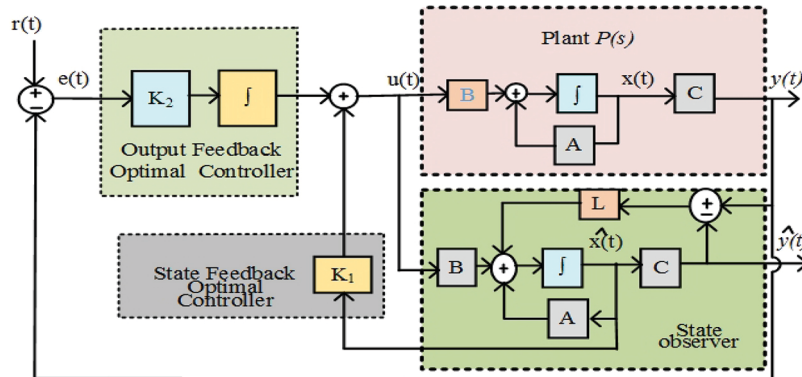


Figure 4: The robust optimal controller with state observer.

3.4.1 Stability of an uncertain system

By considering the continues time linear system represented with the differential equation is given as

$$dx(t)/dt = \mathbf{Ax}(t) = x_0\mathbf{A}_0(t) + x_1\mathbf{A}_1(t) + x_2\mathbf{A}_2(t) + \dots + x_n\mathbf{A}_n(t) \quad (37)$$

The system is stable (i.e all trajectories converge to zero) if and only if there exists a positive definite matrix $\mathbf{P} > 0$ such that

$$\mathbf{V}(\mathbf{x}) = \mathbf{x}^T(t)\mathbf{Px}(t) > 0 \quad \forall \mathbf{x} \neq 0 \quad (38)$$

and satisfies the condition

$$\dot{\mathbf{V}}(\mathbf{x}) = \mathbf{x}^T(t)(\mathbf{A}^T\mathbf{P} + \mathbf{PA})\mathbf{x}(t) < 0 \quad \forall \mathbf{x} \neq 0 \quad (39)$$

The above conditions are called a Lyapunov inequality on \mathbf{P} which is a special form of the LMI. The uncertainty may be because of parameter variation and external disturbance. The system matrices \mathbf{A} and \mathbf{B} can be represented with $\mathbf{A}(p)$ and $\mathbf{B}(p)$ respectively considering the uncertainty in the system. The uncertain matrices $\mathbf{A}(p)$ and $\mathbf{B}(p)$ can be expressed in terms of scalar and structure of uncertainty

$$\mathbf{A}(p) = \mathbf{A}_0 + \sum_{i=1}^N p_i \mathbf{A}_i \quad (40)$$

$$\mathbf{B}(p) = B_0 + \sum_{i=1}^N p_i B_i \quad (41)$$

where A_0 is the normal state matrix, B_0 is the normal input, and p_i is the scalar of the uncertain parameter corresponding uncertain structure matrices A_i and B_i . The range of scalar p_i , structure matrices A_i and B_i are considered as in [23]. The necessary and sufficient condition to satisfy the uncertain system is quadratically stable is

$$\begin{aligned} \dot{V}(x) &= x^T(t)(\mathbf{A}^T(p)\mathbf{P} + \mathbf{P}\mathbf{A}(p))x(t) < 0 \\ \forall x &\neq 0; \end{aligned} \quad (42)$$

The matrix \mathbf{P} must be found to satisfy the system is quadratically stable and it can be solved by the convex optimization method using an LMI inequality. The convex optimization method which can be implemented using MATLAB, not only to assure stability robustness but also to solve the LMIs that arises in the LQR. The robust LQR is formulated while consider the system uncertainty state space model by replacing the matrices \mathbf{A} and \mathbf{B} with the uncertain matrices $\mathbf{A}(p)$ and $\mathbf{B}(p)$.

3.4.2 Design of OSRLQR controller with an LMI approach

For the given system presented in eq. (25), the optimal robust LQR optimization gives the state feedback gain matrix \mathbf{K} for the control input ($u(t) = -\mathbf{K}x(t)$) that reduce a performance index

$$J = \int_0^\infty (x^T(t)\mathbf{Q}x(t) + u^T(t)\mathbf{R}u(t))dt \quad (43)$$

where \mathbf{Q} is a positive semi-definite symmetric matrix and \mathbf{R} is a positive definite symmetric matrix, and the pair (\mathbf{A}, \mathbf{B}) is controllable. Any system with the conventional LQR controller has a percentage of error and overshoots which are undesirable performance. Hence, the robust LQR controller uses the feedback synthesis via Lyapunov functions and reduced into a standard convex problem involving LMI algorithms. The robust LQR is obtained by using the state feedback gain matrix \mathbf{K} such that, the closed loop performance index is given in eq. (44).

$$J = \int_0^\infty (x^T(t)(\mathbf{Q} + \mathbf{K}^T\mathbf{R}\mathbf{K})x(t))dt \quad (44)$$

By using the operator trace ($\text{Tr}(\cdot)$) which assures $\mathbf{A}^T\mathbf{x}\mathbf{B} = \text{Tr}(\mathbf{x}\mathbf{B}\mathbf{A}^T)$, then performance index is equal to the equation given in eq. (45)

$$J = \int_0^\infty \text{Tr}((\mathbf{Q} + \mathbf{K}^T\mathbf{R}\mathbf{K})x(t)x(t)^T)dt \quad (45)$$

$$= \text{Tr}((\mathbf{Q} + \mathbf{K}^T\mathbf{R}\mathbf{K})P) \quad (45)$$

Where $\mathbf{P} = \int_0^\infty x(t)x(t)^T dt$ and this \mathbf{P} will satisfy the condition given in (46)

$$(\mathbf{A} - \mathbf{B}\mathbf{K})\mathbf{P} + \mathbf{P}(\mathbf{A} - \mathbf{B}\mathbf{K})^T + \mathbf{x}_0\mathbf{x}_0^T = 0 \quad (46)$$

where \mathbf{x}_0 represents the initial state. The robust optimal control gain matrix \mathbf{K} can be found by the minimization of the following equation

$$\min_{\mathbf{P} \mathbf{K}} \text{Tr}(\mathbf{Q}\mathbf{P}) + \text{Tr}(\mathbf{R}^{1/2}\mathbf{K}\mathbf{P}\mathbf{K}^T\mathbf{R}^{1/2}) \quad (47)$$

subjected to $(\mathbf{A} - \mathbf{B}\mathbf{K})\mathbf{P} + \mathbf{P}(\mathbf{A} - \mathbf{B}\mathbf{K})^T + \mathbf{x}_0\mathbf{x}_0^T < 0$

The eq. (47) is not linear because of the multiplication of variable matrices \mathbf{P} and \mathbf{K} . So the eq. (47) is converted to linear equation by introducing a new variable matrix $\mathbf{Y} = \mathbf{K}\mathbf{P}$

$$\min_{\mathbf{P} \mathbf{Y}} \text{Tr}(\mathbf{Q}\mathbf{P}) + \text{Tr}(\mathbf{R}^{1/2}\mathbf{Y}\mathbf{P}^{-1}\mathbf{Y}^T\mathbf{R}^{1/2}) \quad (48)$$

subjected to $\mathbf{A}\mathbf{P} + \mathbf{P}\mathbf{A}^T + \mathbf{B}\mathbf{Y} + \mathbf{Y}^T\mathbf{B}^T + \mathbf{x}_0\mathbf{x}_0^T < 0$

The inequality $(\mathbf{A} - \mathbf{BK})\mathbf{P} + \mathbf{P}(\mathbf{A} - \mathbf{BK})^T + \mathbf{x}_0\mathbf{x}_0^T < 0$ is homogeneous in \mathbf{P} and \mathbf{Y} , i.e for any matrices \mathbf{P}^* and \mathbf{Y}^* satisfying the eqs (47) & (48), $\mu\mathbf{P}^*$ and $\mu\mathbf{Y}^*$, with $\mu > 0$, will also fulfill the inequality. The gain $\mathbf{K} = \mathbf{Y}\mathbf{P}^{-1}$ will not depend on the magnitude of μ . It is shown that the nonlinear term $Tr(\mathbf{R}^{1/2}\mathbf{Y}\mathbf{P}^{-1}\mathbf{Y}^T\mathbf{R}^{1/2})$ can be replaced by a second auxiliary variable matrix \mathbf{X} .

$$\min_{\mathbf{X}} Tr(\mathbf{X}) \quad (49)$$

$$\text{Subjected to } \mathbf{X} > (\mathbf{R}^{1/2}\mathbf{Y}\mathbf{P}^{-1}\mathbf{Y}^T\mathbf{R}^{1/2})$$

which, in turn, can dissolve by schur's complement given in eq. (50)

$$\mathbf{X} > (\mathbf{R}^{1/2}\mathbf{Y}\mathbf{P}^{-1}\mathbf{Y}^T\mathbf{R}^{1/2}) \leftrightarrow \begin{pmatrix} \mathbf{X} & \mathbf{R}^{1/2}\mathbf{Y} \\ \mathbf{Y}^T\mathbf{R}^{1/2} & \mathbf{P} \end{pmatrix} > 0 \quad (50)$$

therefore, the absolute LMI formulation of the robust LQR problem is expressed as

$$\min_{\mathbf{P} \in \mathbf{Y} \in \mathbf{X}} Tr(\mathbf{QP}) + Tr(\mathbf{X}) \quad (51)$$

$$\text{subjected to } \mathbf{AP} + \mathbf{PA}^T + \mathbf{BY} + \mathbf{Y}^T\mathbf{B}^T + < 0 \begin{pmatrix} \mathbf{X} & \mathbf{R}^{1/2}\mathbf{Y} \\ \mathbf{Y}^T\mathbf{R}^{1/2} & \mathbf{P} \end{pmatrix} > 0 \mathbf{P} > 0$$

Once the minimization under these constraints is achieved, the optimal robust LQR controller can be obtained by $\mathbf{K} = \mathbf{Y}\mathbf{P}^{-1}$. The optimized gain matrix \mathbf{K} of the robust LQR controller is obtained based on the LQR optimization with an LMI approach.

The advantage of LMI-LQR formulation is the trade-off robustness among the stability and performance robustness for different types of uncertainty.

4 Simulation results

The grid-connected and island mode operation of DG system with OSRLQR controller is performed using MATLAB /SIMULINK/Robust Tool-box. The objective of this study is to supply a quality power to loads during variations in the load, irradiance, and during connecting or disconnecting with the main grid. The performance of th OSRLQR controller for different operation scenarios such as load variation, irradiance changes, mode transition is compared with conventional PI controller. The system parameters used for simulations are listed in Table 1, where f_s , f , $V_{g,abc}$ and V_{dc} are the switching frequency of the inverter, system frequency, line-line grid voltage and DC link voltage respectively.

Table 1: System parameters.

System parameters	Value	System parameters	Value
$V_{g,abc}$	22kV	PCC Voltage	400V
f_s	1.6kHz	w_g	314 rad/s
Filter resistance	$R_1 = R_2 = 0.01$; $R_f = 0.01\Omega$	Filter inductance	$L_1 = L_2 = 0.4mH$
Filter capacitance	C=156.9 μF	f	50Hz
PV power	100kW	V_{dc}	770V

4.1 Grid connected mode

The OSRLQR controlled DG system shown in Figure 1 is designed to supply 100 kW active and 25 KVAR reactive power with standard test conditions applied to PV array i.e., 1000 W/m² and 25°C. The performance of the proposed OSRLQR controller is verified with different load and irradiance variation as shown in the Figure 5. Initially, the DG is operated in the grid-connected mode to supply the load of 50 kW and 10 kVAR and the grid. A load of 250 kW and 100 kVAR is added to initial load between 0.3 s to 0.4 s. The irradiance of the PV array is decreased to 200 W/m² between 0.5 s to 0.75 s. A nonlinear load of 300 kW is added between

0.85 s to 0.9 s and a sudden transient load is added between 0.96 s to 0.962 s. Figure 5(a) shows the variation of solar PV irradiance and Figure 5(b) and (c) shows the active and reactive power of the DG for the different load and irradiance variations. The DC link voltage and voltage across the load is maintained constant for any load and irradiance variations, the same is verified using simulation results shown in Figure 5(d) and (e). The active power tracking (I_d tracking error) and reactive power tracking (I_q tracking error) is perfect with zero error for any variations and it is verified with simulation results are shown in Figure 5(f) and (g). The comparative result for the power, voltage and error tracking shows that OSRLQR controller gives superior robust performance than PI controller during different load and irradiance variations in grid-connected mode.

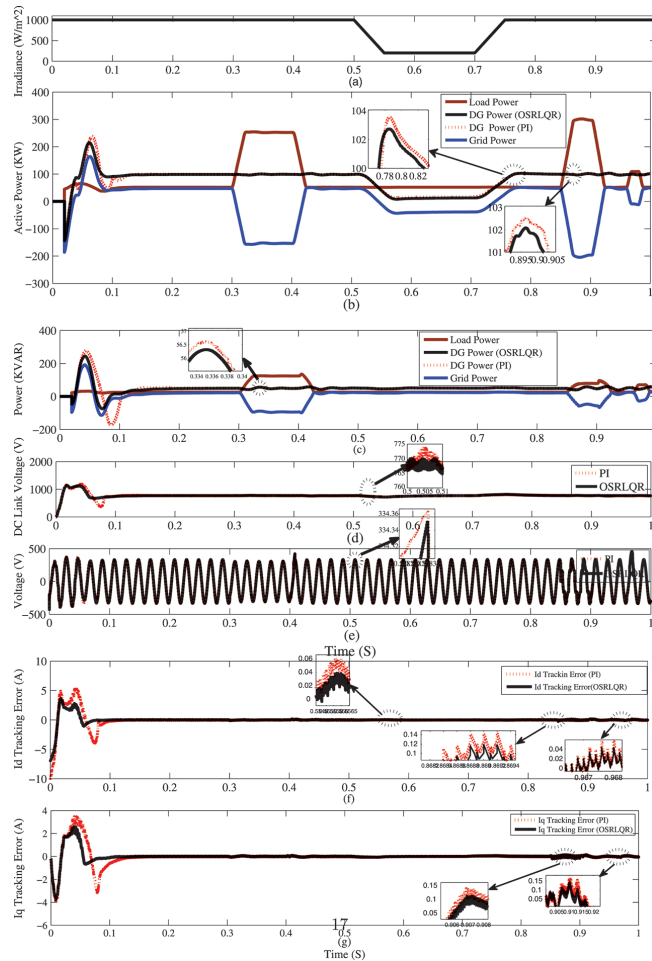


Figure 5: Grid connected mode results with PI and OSRLQR controller, (a) Irradiation (b) Active power(c) Reactive power (d) DC link voltgae (e) PCC Voltage (f) I_d Tracking error (g) I_q Tracking error.

4.2 Transition from grid-connected to Island mode

The DG interfacing inverter system was operated in the grid-connected mode initially and a grid side fault is being created at 1.5 s to test the performance of the detection algorithm. Consequently, the island detection algorithm executes a signal for circuit breaker and mode selection switch. When the DG is disconnected from the grid, it operates in the island mode. Figure 6(a) shows the voltage across the load during the mode switching and a constant voltage is observed throughout the process. The grid and load current are shown in Figure 6(b) and (c) respectively. Figure 6(d) and (e) show the power variations when transferring from grid-connected mode to island mode. The voltage, current, and power satisfy all the requirements during the transition. The results obtained using proposed controller are compared with PI controller and the observation claims that the better performance is achieved using OSRLQR, when the system is transferring from grid-connected mode to island mode.

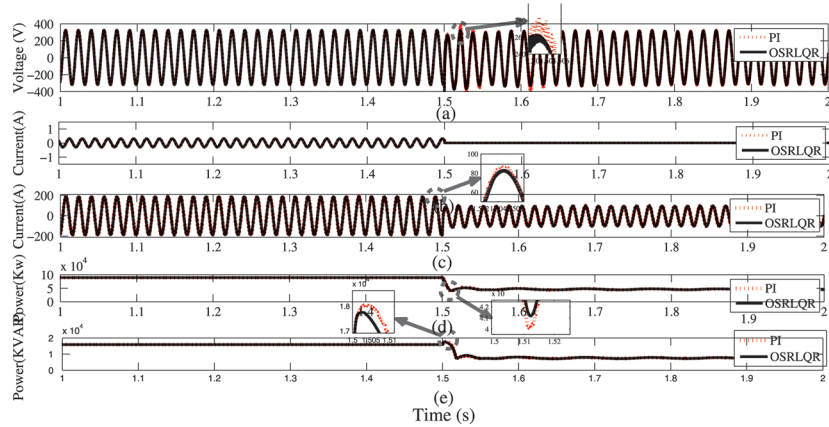


Figure 6: Transition from the grid-connected mode to island mode. (a) Voltage across the critical load (b) Grid current (c) DG current (d) Active power (e) Reactive power.

4.3 Load shedding

This section explains the performance of the load shedding algorithm applied for islanded DG system in the presence of the OSRLQR controller. The load shedding algorithm is implemented to maintain the magnitude of PCC voltage within the normal operating range when the power mismatch occurs in island mode and the corresponding results are presented in Figure 7(a) and (b). The load in this test scenario is taken as 150kW and 20 KVAR, but the DG supplies 100kW and 20 KVAR, and the remaining load is supplied by the utility grid in grid connected condition. When the DG is disconnected from the grid at 1.5 s, the total load demand is beyond the DG capacity. The voltage transient or fall in voltage appears due to the power mismatch. On the situation, when the voltage is not within normal operating range then the load shedding algorithm comes into action and disconnects some part of the load.

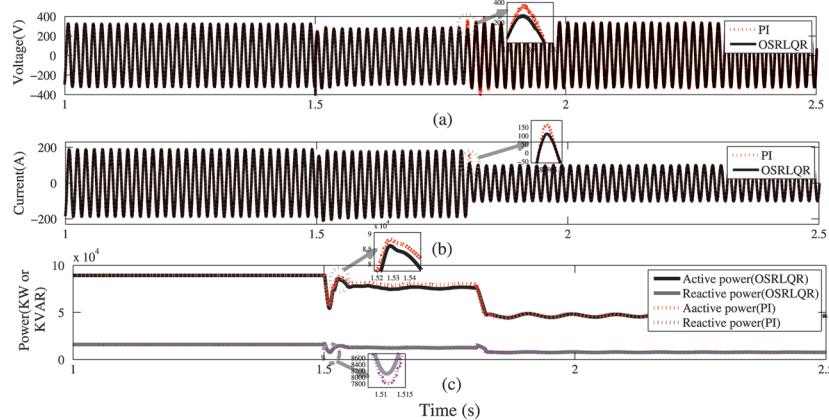


Figure 7: Transition from the grid connected mode to the island along load shedding. (a) The PCC voltage across the load (b) DG current (c) Active and reactive power.

4.4 Island mode

Initially, the DG in island mode with OSRLQR controller supplies the power to the load of 100 kW and 10 kVAR. A load of 30 kW and 10 kVAR added between the 0.3 s to 0.5 s and a sudden load of 100 kW and 10 kVAR is added between 0.85 s to 0.86 s. The DC link voltage which is maintained constant with DC side Boost controller and observed in Figure 8(a). The frequency is observed in Figure 8(b) and it is maintained at 50 Hz during load variations. Figure 8(c) shows the active and reactive power of the DG in island mode for different load variations. The obtained results convey the better robust performance of OSRLQR controller compared to PI controller during load variations. Figure 8(d) shows the PCC voltage for different load variations and the tracking error in terms of the I_d and I_q is observed to be zero which can be seen in Figure 8 (e) and (f). The island mode result shows the better robust performance of the OSRLQR controller compared to PI controller for the different loads.

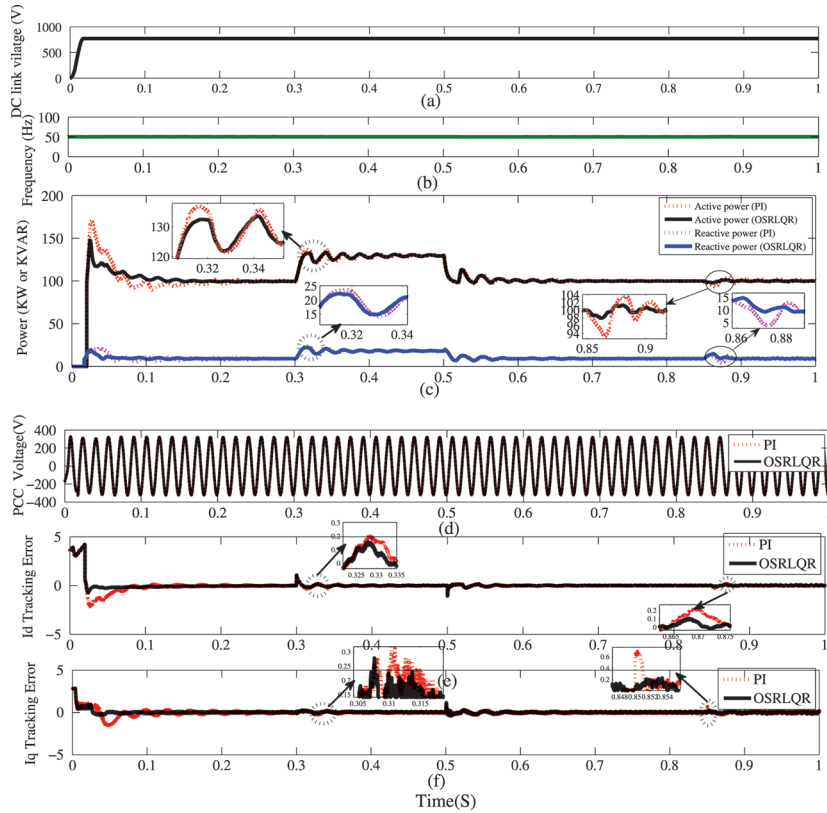


Figure 8: Island mode results with PI and OSRLQR controller (a) DC Link Voltage (b) Frequency (c) Active and Reactive power (d) PCC Voltage (e) I_d Tracking error (f) I_q Tracking error.

4.5 Transition from Island to grid-connected mode

This section presents the DG re-connection to the grid from island mode using synchronization algorithm. Initially, the DG operates in the island mode up to 1.5 s and supplies the load of 50 kW and 10 KVAR. At 1.5 s, both DG interfacing inverter output and grid are synchronized for reconnection.

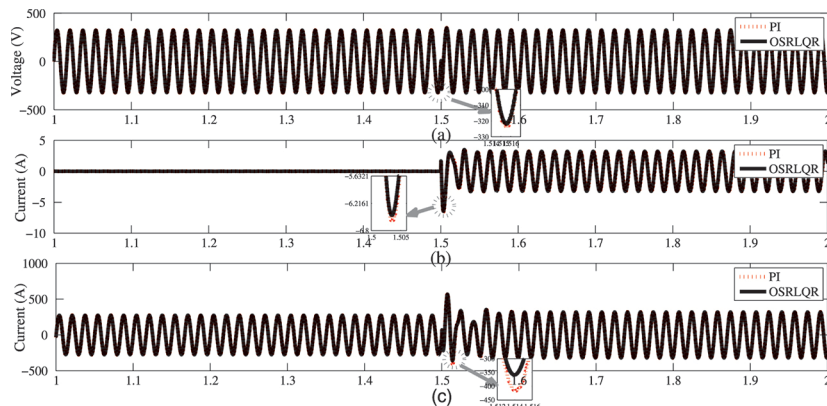


Figure 9: Transition from the island mode to the grid-connected mode using grid synchronization algorithm (a) Voltage (b) Grid current (c) DG current.

Figure 9(a),(b)&(c) shows the voltage across local load, grid injected current and load current respectively. The observation claims that the PCC voltage is maintained constant in the islanded, grid-connected and during transition modes.

5 Experimental results

An experimental setup of the DG inverter system is developed to certify the practical feasibility of the proposed OSRLQR control scheme. The experimental setup is built with fewer changes of the actual proposed DG inverter with OSRLQR control scheme and it is shown in Figure 10. The experimental setup consists the PV panels, boost converter along with MPPT control, bi-directional inverter along with real-time control scheme using dSPACE. The experimental test is conducted with system parameters as a DC-link voltage $V_{DC} = 500V$, $V_{abc} = 400V$, LCL-filter $L_1 = 1mH$, $L_2 = 0 : 5mH$ and $C_f = 10F$. The proposed control have been implemented for the real-time system using dSPACE control desk software and dSPACE RTI 1202. The real-time measurements and feedbacks are obtained by the current and voltage sensors and this feedbacks have been sent to the proposed scheme through dSPACE RTI 1202. The real-time SPWM pulses which are generated by the proposed scheme through dSPACE are given to the power converter. The output of the DC-DC converter is connected to three-phase IGBT based VSI across a DC-link capacitor of $600\mu F$ and inverter output power is fed to load or grid through LCL filter. The experimental control performance of the proposed control scheme is analyzed separately for the grid-connected, islanded and transition modes. Each experimental result the DG system under OSRLQR controller is compared with the result of the same system under the PI controller. In grid connected and islanded mode the results comparison is observed using THD of the DG output voltage and current. The experimental DG output voltage and current in grid-connected mode are shown in Figure 11. The experimental grid connected to islanded transition mode results are shown in Figure 12. The results shown in Figure 13 and Figure 14 indicates the DG output voltage and current in island mode and islanded to grid-connected transition mode. The experimental results demonstrate the superiority of proposed control scheme over the conventional control scheme.

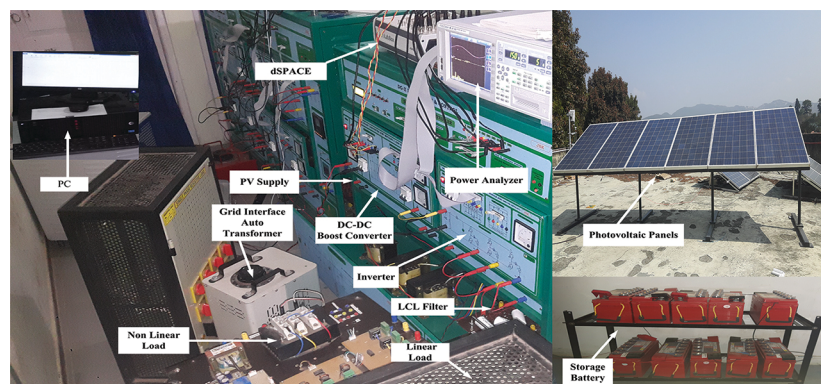


Figure 10: Experimental setup.

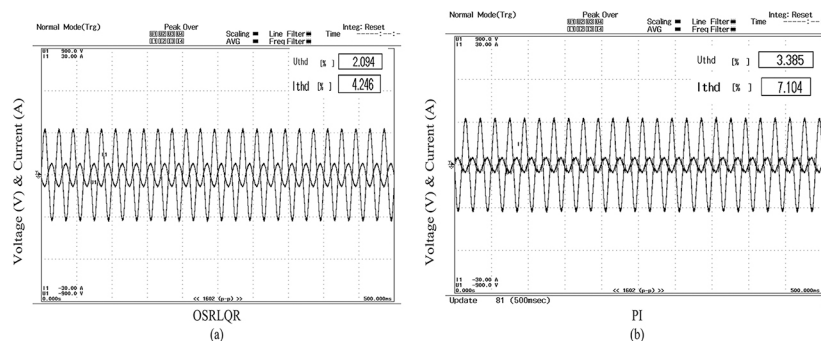


Figure 11: Experimental DG output voltage and current in grid connected mode (a) OSRLQR controller, (b) PI controller.

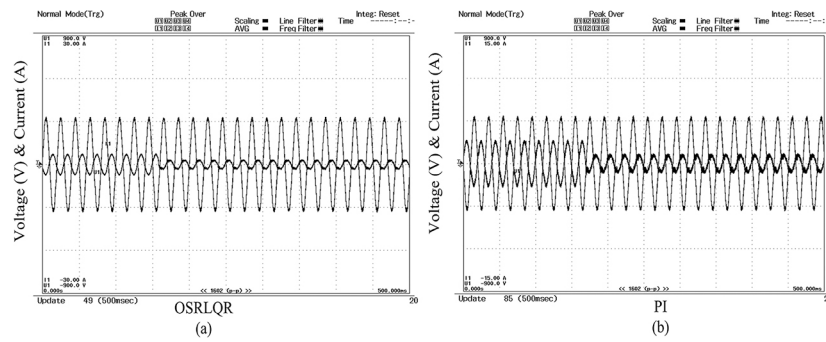


Figure 12: Experimental DG output voltage and current in the grid connected to islanded transition mode (a) OSRLQR controller, (b) PI controller.

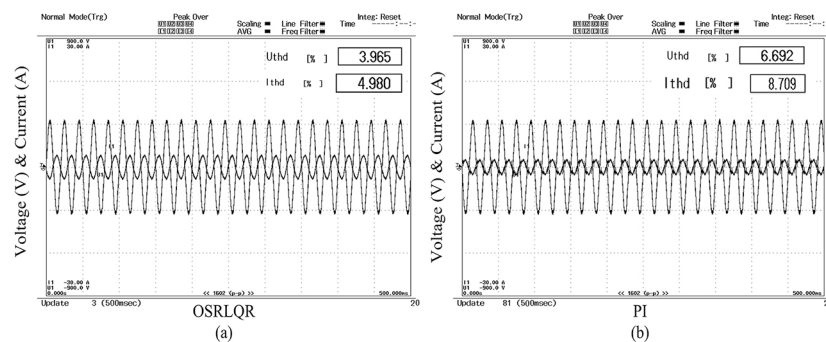


Figure 13: Experimental DG output voltage and current in islanded mode (a) OSRLQR controller, (b) PI controller.

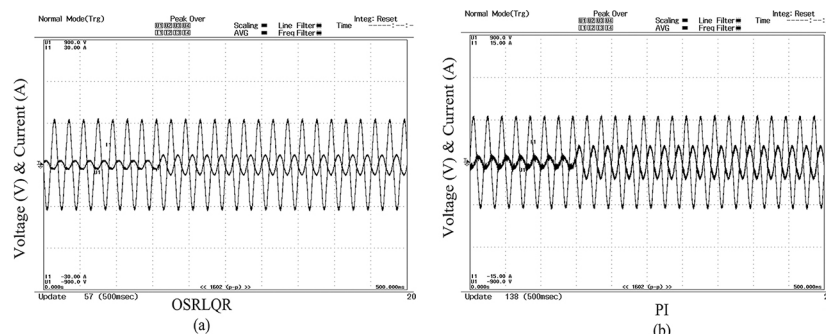


Figure 14: Experimental DG output voltage and current in the islanded to grid-connected transition mode (a) OSRLQR controller, (b) PI controller.

6 Conclusion

In this paper, a robust LQR controller with an LMI approach has been analyzed to control the DG system in grid-connected as well as in islanded mode. The proposed OSRLQR controller with the system states which are replicated by the observer and the output feedback error states has been implemented along with separate reference generation technique for both the modes. The control performance of the OSRLQR controller is observed for linear, nonlinear, transient load and variable irradiance conditions. It is also evident from the result that the variation in voltages and currents are within the acceptable limit even during transition from grid-connected to islanded mode and vice versa. The results also confirm that the proposed controller gives better performance compared to PI controller in terms of active power, reactive power, PCC voltage, load current, DC-link voltage and tracking error. The seamless transition from the grid connected mode to island mode and vice versa is achieved using island detection, load shedding, and grid synchronization techniques. The superiority of the proposed control approach compared to the conventional PI controller is verified with simulation results and the practical feasibility of the proposed control scheme is validated with experimental prototype developed in the laboratory. The proposed OSRLQR controller with uncertainty model is satisfactory for the inherent trade-off robustness between the stability and performance during grid-connected, islanded, and transition of modes.

Funding

This work is supported by the REC Transmission Projects Company Limited Grant RECTPCL/CSR/2016-17/693, India.

References

- [1] Blaabjerg F, Teodorescu R, Liserre M, Timbus AV. Overview of control and grid synchronization for distributed power generation systems. *IEEE Trans Indust Electron.* 2006;53:1398–409.
- [2] Islam MS, Raju NI, Ahmed AU. Sinusoidal PWM signal generation technique for three phase voltage source inverter with analog circuit & simulation of PWM inverter for standalone load & micro-grid system. *Int J Renewable Energy Res.* 3: 647–58.
- [3] Hohm DP, Ropp ME. Comparative study of maximum power point tracking algorithms using an experimental, programmable, maximum power point tracking test bed. Conference Record of the Twenty-Eighth, IEEE Photovoltaic Specialists Conference-2000, 2000: 1699–702.z
- [4] Beres RN, Wang X, Liserre M, Blaabjerg F, Bak CL. A review of passive power filters for three-phase grid-connected voltage-source converters. *IEEE J Emerg Sel Top Power Electron.* 2016;4:54–69.
- [5] Puhan PS, Ray PK and Panda G. Development of real time implementation of 5/5 rule based Fuzzy logic controller shunt active power filter for power quality improvement. *Int J Emerg Electr Power Syst.* 2016;17:607–17.
- [6] Babu BC, Anurag A, Sowmya TN, Marandi D. Decoupled control strategy of grid interactive inverter system with optimal LCL filter design. *Int J Emerg Electr Power Syst (ISI Indexed)* 2013;14:477–86.
- [7] Reznik A, Simes MG, Al-Durra A, Muyeen SM. Filter design and performance analysis for grid-interconnected systems. *IEEE Trans Ind Appl.* 2014;50:1225–32.
- [8] Park S, Chen C, Lai J, Moon S. Admittance compensation in current loop control for a grid-tie LCL fuel cell inverter. *IEEE Trans Power Electron* 2008;23:1716–23.
- [9] Balaguer IJ, Lei Q, Yang S, Supatti U, Peng FZ. Control for grid-connected and intentional Islanding operations of distributed power generation. *IEEE Trans Ind Electron.* 2011;58:147–57.
- [10] Golestan S, Guerrero JM, Vasquez JC. Three-Phase PLLs: a review of recent advances. *IEEE Trans Power Electron.* 2017;32:1894–907.
- [11] Egea-Alvarez A, Junyent-Ferr A, Gomis-Bellmunt O. Active and reactive power control of grid connected distributed generation systems. In: Proceedings of Modeling and Control of Sustainable Power Systems, 2012: 47–81.
- [12] Liu L, Li H, Xue Y, Liu W. Decoupled active and reactive power control for large-scale grid-connected photovoltaic systems using cascaded modular multilevel converters. *IEEE Trans Power Electron.* 2015;30:176–87.
- [13] Liang M, Zheng TQ. Synchronous PI control for three phase grid connected Photovoltaic inverter. In: Chinese Control and Decision Conference(CCDC), 2010: 2302–7.
- [14] Goncalves AFQ, Aguiar CR, Bastos RF, Pozzebon GG, Machado RQ. Voltage and power control used to stabilize the distributed generation system for stand-alone or grid-connected operation. *IET Power Electron.* 2016;9:491–501.
- [15] Jiang Z, Yu X. Active power-voltage control scheme for islanding operation of inverter-interfaced micro grids. In: IEEE Power & Energy Society General Meeting, Calgary, AB, 2009: 1–7.
- [16] Wang TCY, Ye Z, Sinha G, Yuan X. Output filter design for a grid-interconnected three-phase inverter. In: Power Electronics Specialist Conference, PESC '03. 2003 IEEE 34th Annual, 2003: 779–84, vol. 2.
- [17] Liserre M, Teodorescu R, Blaabjerg F. Multiple harmonics control for three-phase grid converter systems with the use of PI-RES current controller in a rotating frame. *IEEE Trans Power Electron.* 2006;21:836–41.
- [18] Gabe IJ, Massing JR, Montagner VF, Pinheiro H. Stability analysis of grid-connected voltage source inverters with LCL-filters using partial state feedback. In: Proceeding of the European Conference on Power Electronics and Applications (EPE), 2007: 1–10.
- [19] Gabe IJ, Montagner VF, Pinheiro H. Design and implementation of a robust current controller for VSI connected to the grid through an LCL filter. *IEEE Trans Power Electron.* 2009;24:1444–52.
- [20] Prez-Ibacache R, Silva C, Yazdani A.. Linear state-feedback primary control for enhanced dynamic response of AC microgrids. *IEEE Trans Smart Grid* 2018. DOI: 10.1109/TSG.2018.2818624
- [21] Dirscherl C, Fessler J, Hackl CM, Ipach H. State-feedback controller and observer design for grid-connected voltage source power converters with LCL-filter. In IEEE Conference on Control Applications (CCA), Sydney, NSW, 2015: 215–22.
- [22] Olalla C, Leyva R, El Aroudi A, Queinnec I. Robust LQR control for PWM converters: an LMI approach. *IEEE Trans Ind Electron.* 2009;56:2548–58.
- [23] Douglas J, Athans M. Robust linear quadratic designs with real parameter uncertainty. *IEEE Trans Autom Control.* 1994;39:107–11.
- [24] Hernandez-Gonzalez G, Iravani R. Current injection for active islanding detection of electronically-interfaced distributed resources. *IEEE Trans Power Del.* 2006;21:1698–705.
- [25] Thacker T, Wang F, Burgos R, Boroyevich D. Islanding detection using a coordinate transformation based phase-locked loop. In: Proceedings of the IEEE PESC, June 2007: 1151–6.
- [26] Lopes LAC, Zhang YZ. Islanding detection assessment of multiinverter systems with active frequency drifting methods. *IEEE Trans Power Del.* 2008;23:480–6.
- [27] Pinto SJ, Panda G. Performance assessment of islanding detection using complex wavelet in a three-phase utility interactive inverter system. In: IEEE PES Asia-Pacific Power and Energy Engineering Conference (APPEEC), Bangalore, 2017: 1–6.
- [28] Shaikh F, Joseph B. Simulation of synchronous reference frame PLL for grid synchronization using Simulink. In: International Conference on Advances in Computing, Communication and Control (ICAC3), Mumbai, 2017: 1–6.

- [29] Teodorescu R, Blaabjerg F. Flexible control of small wind turbines with grid failure detection operating in stand-alone and grid-connected mode. *IEEE Trans Power Electron.* 2004;19:1323–32.
- [30] Krishnan G, Gaonkar DN. Intentional islanding operations of distributed generation systems with a load shedding algorithm. In: *IEEE International Conference on Power Electronics, Drives and Energy Systems (PEDES)*, Bengaluru, 2012: 1–6.
- [31] Laghari JA, Mokhlis H, Bakar AHA, Mohamad H. Application of computational intelligence techniques for load shedding in power systems: a review. *Energy Convers Manage* 2013;75:130.
- [32] Liu G, Xiao B, Starke M, Ceylan O, Tomsovic K. A robust load shedding strategy for microgrid islanding transition. In: *IEEE/PES Transmission and Distribution Conference and Exposition (TD)*, Dallas, TX, 2016: 1–5.